

Investigation of the Adherence Influence on the Dynamic Behavior of the Vehicle

Nacer Hamadi¹, Djamel-eddine Ameddah¹ and Hocine Imine²

¹*Department of Electronic, Advanced Electronic Laboratory (A.E.L.)
Faculty of technologies, Batna University, Alegria
nacer.hamadi@univ-batna.dz, Abida_dj@live.fr*

²*French institute of Sciences and Technologies of Transport, Installation and the
Networks, University Paris-East, LEPSIS, IFSTTAR, France
hocine.imine@ifsttar.fr*

Abstract

In this paper, we were interested on the adherence influence on the dynamic behavior of the vehicle. With this intention, we based ourselves on a articulated nominal dynamic model of a ground vehicle as well as the contact tire-road.

Keywords: *vehicle; modeling; tire; road; adherence; simulation; Lagrange formalism*

1. Introduction

A vehicle is a nonlinear complex system with its kinematics and dynamic characteristics (actuators, thermal engine); moreover, and particularly in all ground, it can be subjected to many disturbances, such as changes of adherence of the ground or slope, strong gales, *etc.*

In this paper, one will be interested in the study of the adherence influence on the dynamic behavior of the vehicle for the various types of lanes [1-3]. For this study, we used the structure defined by the diagram of the Figure 1. The structure is based mainly on the direct dynamic model of the physical model more precise and realistic than the bicycle model or quarter model used usually for some control purposes developed in [7-12] and the entries such as the orders of the driver (flying, accelerating, brake), the aerodynamics effects and the road entries.

Indeed, the adherence influence represents the effects between the tire and the ground; these effects on the level of the contacts points enter in all the dynamic exchanges, which condition the handling of the vehicle. The major part of the efforts applied to the vehicle pass through the tires, which depend on the type and the carriageway surfacing.

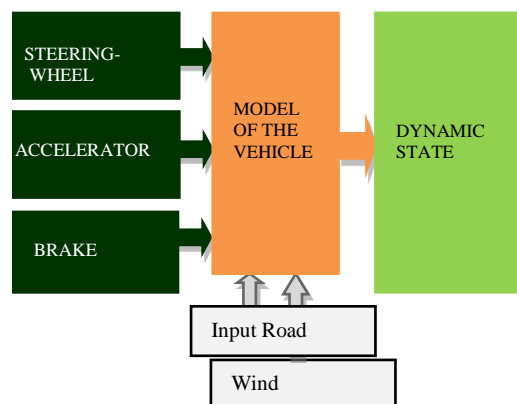


Figure 1. Diagram Simulator of the Vehicle

In this paper we employed the empirical formula suggested by Bakker and Pacejka [13] to describe the behavior of the tire. We will concentrate on models who take account of the factors of environment (load, nature of the roadway) or of the intrinsic properties of the tire (structure of the tire, rigidity, pressure). To represent, the tire longitudinal and side behavior in the nonlinear case, the formula of Pacejka makes it possible to define by the same basic formula the longitudinal force, the lateral force and the self-aligning torque under conditions of pure sideslip or pure braking expressed in the pneumatic reference. The parameters on which these functions depend are sideslip, longitudinal slip, the camber angle and the vertical load. If we base on the results of a test carried out for tires coefficients Pacejka measured by ARIANE within the IFSTTAR (ex LCPC 1), for the dryness and wet lanes to calculate the longitudinal and side contacts forces.

This paper is organized as follows; In the second part, we present the modeling of the vehicle, in the third part, we discuss and analyze the results of simulation, and an experimental validation is shown, in particular by the results of the influence of the adherence on the dynamic behavior of the vehicle. Finally, a conclusion and some prospects are given in the last part.

2. Vehicle Modelling

2.1. Vehicle Frame

To calculate the operational dynamic model, simplifications related to the dynamic structure of the vehicle are essential:

- The chassis is regarded as a rigid 3d body
- Each wheel is regarded as a rigid disk and it is assumed to be represented by a single point of contact with the terrain surface.
- The steering of the direct wheels, clearances of the suspensions and the rotation of the wheels can represent the kinematics of connection tire/road.

The Figure 2 illustrates all the kinematics joints considered in the used model.

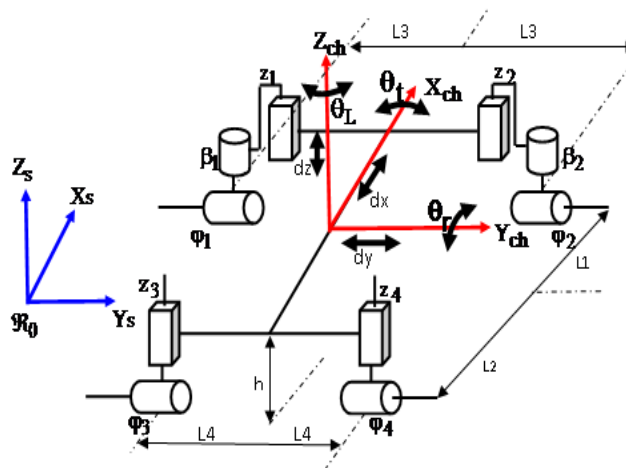


Figure 2. Coordinate System to describe the Vehicle Motion

The nominal dynamic model considered with 16 DoF is divided like following:

- The Frame with 6 DoF accounts of three translator movements (x , y , z) and three

rotational movements rolling-pitching-yaw $\theta_r, \theta_l, \theta_i$ according to three axes' x y z The suspension with 4DoF represents 4 variables of clearances (z_1, z_2, z_3, z_4).

- The direction with 2 DoF respectively represents the steering angles left and right of the front steer wheels (β_1, β_2).
- The wheels with 4 DoF represents the rotation angles of the four wheels around the fused axis ($\varphi_1, \varphi_2, \varphi_3, \varphi_4$).

The generalized coordinate's variable vector $q \in \mathbb{R}^{16}$ defined by:

$$q^T = [x, y, z, \theta_r, \theta_l, \theta_i, z_1, z_2, z_3, z_4, \beta_1, \beta_2, \varphi_1, \varphi_2, \varphi_3, \varphi_4]$$

The dynamic parameters considered are the mass of the chassis MS, the mass of each front wheel MRF, the mass of each rear wheel MRR, and h1 and h2 is the initial length spring of the front suspension and h3 and h4 is the initial length spring of the rear suspension.

2.2. Dynamic Model

The dynamic model of the vehicle is obtained by using the approach of Lagrange based on the calculation of the kinetic and potential energy of the complete system. The motion equation of the mechanism is given by:

$$M(q)\ddot{q} + C(q, \dot{q})\dot{q} + G(q) = \Gamma \quad (1)$$

$\Gamma = \tau_m + \tau_D - \tau_{rr} - \tau_{susp} + \Gamma_a$ is the vector of the internal and external forces between the vehicle bodies. Where τ_m represent the engine torque of the two driving wheels, direction torque of the two cap wheels is τ_D , rolling friction torque of the 4 wheels is τ_{rr} , torques of the 4 suspensions is τ_{susp} and Γ_a is the vector of contact forces on each wheel (see section 3).

$Mq \in \mathbb{R}^{16 \times 16}$ Represent the matrix of the kinetic energy, named the inertia system matrix. It is symmetrical, definite and positive. Of these elements, are functions of the joint variables q_i . The total kinetic energy is calculated by the formula:

$$T = \frac{1}{2} \dot{q}^T M(q) \dot{q} \quad (2)$$

And $M(q)$ is given by :

$$M(q) = \sum_{i=1}^5 m_i J_{v_i}^T(q) J_{v_i}(q) + J_{w_i}^T(q) R_i(q) I_i R_i^T(q) J_{w_i} \quad (3)$$

With

$J_{v_i}^T(q)$ Jacobian matrix transposed of the linear velocity for body i,

$J_{w_i}^T(q)$ Jacobian matrix transposed of the angular velocity for body i,

$R_i(q)$ Rotate matrix of body i,

I_i Inertia matrix of body i,

m_i Mass of body i.

To calculate the Jacobian matrix($J_{v_i}^T(q)$ and $J_{w_i}^T(q)$)and rotation matrix $R_i(q)$, we chose, the homogeneous matrix based on the translation and rotation, who define the movement of a body in relation to another, the homogeneous matrix is given by:

$$\begin{bmatrix} \cos\theta_l \cos\theta_r & \sin\theta_l \cos\theta_r + \cos\theta_l \sin\theta_l \sin\theta_r & -\sin\theta_l \sin\theta_r - \cos\theta_l \sin\theta_l \cos\theta_r & dx \\ \cos\theta_l \cos\theta_r & \cos\theta_l \cos\theta_r + \sin\theta_l \sin\theta_l \sin\theta_r & \cos\theta_l \sin\theta_r - \sin\theta_l \sin\theta_l \sin\theta_r & dy \\ \sin\theta_l & -\cos\theta_l \sin\theta_r & \cos\theta_l \cos\theta_r & dz \\ 0 & 0 & 0 & 1 \end{bmatrix}$$

$C(q, \dot{q}) \in R^{16 \times 16}$ Represent the matrix of the Coriolis and Centrifuges terms. It is of dimension (16x16). The calculation of the dynamic coefficients of the matrix $C(q, \dot{q})$ is established by respecting the property of passivity of the system. A way of calculating the coefficients of the matrix is to use the symbols of Christophel.

$$C_{i,j,k} = \frac{1}{2} \left[\frac{\partial M_{kj}}{\partial q_i} + \frac{\partial M_{ki}}{\partial q_j} - \frac{\partial M_{ij}}{\partial q_k} \right] \quad (4)$$

With (i=1...16,j=1..16,k=1...16)

$$C_{kj} = \sum_{i=1}^{16} c_{i,j,k} \dot{q}_i \quad (5)$$

With (k=1...16,j=1..16)

The form symbolic of the matrix $C(q, \dot{q})$ is given in appendix.

$G(q)$ is the vector of the gravity forces; It given by the gradient of the potential energy EP versus to q, The potential energy of the i-th body can be computed by assuming that the mass of the entire object is concentrated at its center of mass and is given by

$$EP_i = g^T r_{ci} m_i \quad (6)$$

Where g is vector giving the direction of gravity in the inertial frame and the vector r_{ci} gives the coordinates of the center of mass of body i. The total potential energy of the 5-body of our system is therefore

$$EP = -g(MS.Z - MRF(h1 + h2 - Z1 - Z2 - 2Z) - MRR.(h3 + h4 - Z3 - Z4 - 2Z)) \quad (7)$$

So

$$G(q) = [0, 0, -g.(MS + 2.MRF + 2.MRR), 0, 0, 0, -g.MRF, -g.MRF, -g.MRR, -g.MRR, 0, 0, 0, 0, 0, 0]^T \quad (8)$$

Finally, the 16 DoF nominal model proposed is then equivalent to:

$$\begin{bmatrix} M_{1,1} & \cdots & M_{1,16} \\ \vdots & \ddots & \vdots \\ M_{16,1} & \cdots & M_{16,16} \end{bmatrix} \begin{bmatrix} \dot{q}_1 \\ \vdots \\ \dot{q}_{16} \end{bmatrix} + \begin{bmatrix} C_{1,1} & \cdots & C_{1,16} \\ \vdots & \ddots & \vdots \\ C_{16,1} & \cdots & C_{16,16} \end{bmatrix} \begin{bmatrix} \dot{q}_1 \\ \vdots \\ \dot{q}_{16} \end{bmatrix} + \begin{bmatrix} G_1 \\ \vdots \\ G_{16} \end{bmatrix} + \tau_{susp} + \tau_{rr} = \Gamma_a + \tau_m \quad (9)$$

The resolution of the mechanism movements is equivalent to solving the following numerically equation [5, 6]:

$$\ddot{q} = M^{-1}(q) [\Gamma - C(q, \dot{q})\dot{q} - G(q)] \quad (10)$$

The equivalent state space representation, Let the state vector is $X^T = (X1^T, X2^T) = (q^T, \dot{q}^T)$ can be written:

$$\begin{cases} \dot{X1} = X2 \\ \dot{X2} = M^{-1} [\Gamma - C(X1, X2) * X2 - G(X1)] + M^{-1} * MPC * X3 \\ y = X1 \end{cases} \quad (11)$$

$$X1 = [x, y, z, \phi_x, \phi_y, \phi_z, z1, z2, z3, z4, \beta_1, \beta_2, \phi_1, \phi_2, \phi_3, \phi_4]$$

$$X2 = [\dot{x}, \dot{y}, \dot{z}, \dot{\theta}_r, \dot{\theta}_l, \dot{\theta}_1, \dot{z}1, \dot{z}2, \dot{z}3, \dot{z}4, \dot{\beta}_1, \dot{\beta}_2, \dot{\phi}_1, \dot{\phi}_2, \dot{\phi}_3, \dot{\phi}_4]$$

$$X3 = [Fx1, Fy1, Fz1, Fx2, Fy2, Fz2, Fx3, Fy3, Fz3, Fx4, Fy4, Fz4]$$

$M(X1) \in \mathbb{R}^{16 \times 16}$ Inertia matrix of the system is a symmetric positive definite

$C(X1, X2) \in \mathbb{R}^{16 \times 16}$ Matrix of centrifugal and Coriolis terms,

$G(X1) \in \mathbb{R}^{16 \times 1}$ is the vector of gravity terms,

$MPC = J^T * MR$ Passage matrix of the 4 points of contacts relatively to the absolute reference,

$J^T \in \mathbb{R}^{16 \times 12}$ Jacobian matrix of the 4 points of contacts,

$MR = \mathcal{R}_i(\psi_x, \psi_y, \psi_z) \in \mathbb{R}^{12 \times 12}$ Rotation matrix of the points of contacts for the plan of the road relatively to absolute reference,

$X3 \in \mathbb{R}^{12}$ represent the forces of the 4-point of contacts; the longitudinal, Side and vertical force, Γ is the vector of the internal and external forces between the vehicle bodies.

2.3. Interaction Wheel-ground

2.3.1. Dynamic Modelling of the Tire: In the case of pure slip, the general form of the basic model proposed to express the expression of the tangential forces is given in ([7, 10, 13]):

$$y(x) = D \sin \left\{ C \arctan \left[Bx - E (Bx - r \tan Bx) \right] \right\} \quad (12)$$

$$Y(x) = Y(X) + S_v$$

$$x = X + S_h$$

The curve obtained by the above equation is represented in the Figure 3, whose pace makes it possible to find easily great number of these parameters:

- B: factor of stiffness
- C: factor of form
- D: value of peak (compared to axis X) (N)
- E: factor of curve
- BCD: rigidity of drift (slope in the beginning)
- S_v, S_x: offset vertical/longitudinal
- x: drift angle (rad)/slip (%)
- y: variable of output (F_x or F_y) (N)

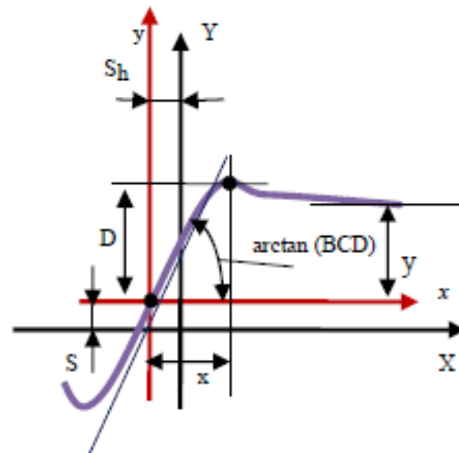


Figure.3. Characteristics of the Pacejka Formula

Like bases of parameter setting of the tires, we have the curves of the following [LCPC] adherences (longitudinal and side) Figure 4:

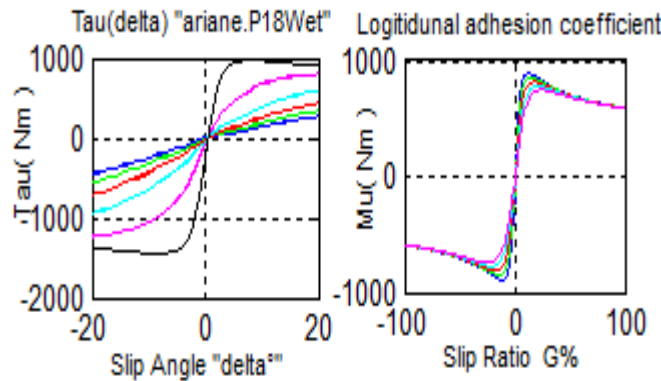


Figure 4. Relationships between Longitudinal and Side Adhesion Coefficient using the Magic Formula

2.3.2. Forces of Tire/Road Contact: The efforts at each contact tire/road are, the longitudinal

force F_{0xi} , the side force F_{0yi} and the normal force F_{0zi} Figure 2.

$$F_{0i} = [F_{0xi}, F_{0yi}, F_{0zi}]^T$$

For the case of the four-wheeled vehicle, the action of the forces of contact on each wheel is expressed by:

$$\Gamma_a = \sum_{i=1}^4 \Gamma_{ai} = J^T F_0 \tag{13}$$

With: $F_0 \in \mathfrak{R}^{12}$ is the vector of the contact forces and $J^T \in \mathfrak{R}^{12 \times 15}$ (see appendix) is the matrix such as:

$$J^T = [J_1^T \ J_2^T \ J_3^T \ J_4^T]$$

$$F_0 = [F_{01}^T \ F_{02}^T \ F_{03}^T \ F_{04}^T]$$

If the plan of the surface of contact wheel / ground forms an angle ψ_x at axis $\overline{Ox_0}$ an angle ψ_y at axis $\overline{Oy_0}$ and an angle ψ_z at axis $\overline{Oz_0}$ then one has:

$$F_{0i} = \mathfrak{R}_i(\psi_x, \psi_y, \psi_z) F_{ci} \tag{14}$$

With $\mathfrak{R}_i(\psi_x, \psi_y, \psi_z)$ is the matrix of rotation of the reference frame of the wheel i whose origin is fixed at the center of the zone of contact, towards the absolute reference frame.

- Steerable wheels

$$R_{i=1,2}(\psi_x, \psi_y, \psi_z) = \begin{bmatrix} \cos(\psi_z + \beta b) \cos(\psi_y) & \sin(\psi_z + \beta b) \cos(\psi_x) + \sin(\psi_y) \sin(\psi_x) \cos(\psi_z + \beta b) \\ \sin(\psi_z + \beta b) \cos(\psi_x) & \cos(\psi_z + \beta b) \cos(\psi_x) + \sin(\psi_y) \sin(\psi_x) \sin(\psi_z + \beta b) \\ \sin(\psi_y) & -\cos(\psi_y) \sin(\psi_x) \\ & -\sin(\psi_z + \beta b) \sin(\psi_x) - \sin(\psi_y) \cos(\psi_x) \cos(\psi_z + \beta b) \\ & -\sin(\psi_z + \beta b) \sin(\psi_x) - \sin(\psi_y) \cos(\psi_x) \cos(\psi_z + \beta b) \\ & \cos(\psi_y) \cos(\psi_x) \end{bmatrix}$$

- No-Steer wheels

$$\left\{ \begin{array}{l} G_i = \frac{Rw_i}{V_{xi}} - 1 \quad \text{if } V_{xi} > Rw_i \\ G_i = 1 - \frac{Rw_i}{V_{xi}} \quad \text{if } Rw_i < V_{xi} \end{array} \right. \quad (15)$$

V_{xi} Is the speed of the wheel center; R is the effective ray of the wheel: when a vertical force as applied to the tire, this one undergoes a crushing, which reduces the ray of the wheel

2.3.5. Sideslip Angle: The mathematical formulas of the sideslip angles, expressed in the reference frame related to the vehicle is given by the system (16) respectively, for the wheels: front-left, front-right, rear-left and rear-right [7].

$$\left\{ \begin{array}{l} \alpha_1 = \beta_b - \frac{V_y + L_1 \dot{\theta}_1}{V_x - L_3 \dot{\theta}_1} \\ \alpha_2 = \beta_b - \frac{V_y + L_1 \dot{\theta}_1}{V_x + L_3 \dot{\theta}_1} \\ \alpha_3 = -\frac{V_y - L_2 \dot{\theta}_1}{V_x - L_4 \dot{\theta}_1} \\ \alpha_4 = -\frac{V_y - L_2 \dot{\theta}_1}{V_x + L_4 \dot{\theta}_1} \end{array} \right. \quad (16)$$

With:

- α_i Sideslip angle of the tire.
- V_y Lateral velocity of the vehicle.
- V_x Longitudinal velocity of the vehicle

2.3.6. Normal Force: The normal forces applied to the tires vary as a function to longitudinal and side accelerations of the vehicle. The expressions of these forces are given by [15]

$$F_N = \frac{Ms}{2 * (L_1 + L_2)} \left(g * L_2 - h * \dot{V}_x \right) \quad (17)$$

\dot{V}_x Is the longitudinal acceleration of the vehicle

2.3.7. Steering-Wheel Angle: The Steering-Wheel angle as chosen as mentioned in the Figure 6.

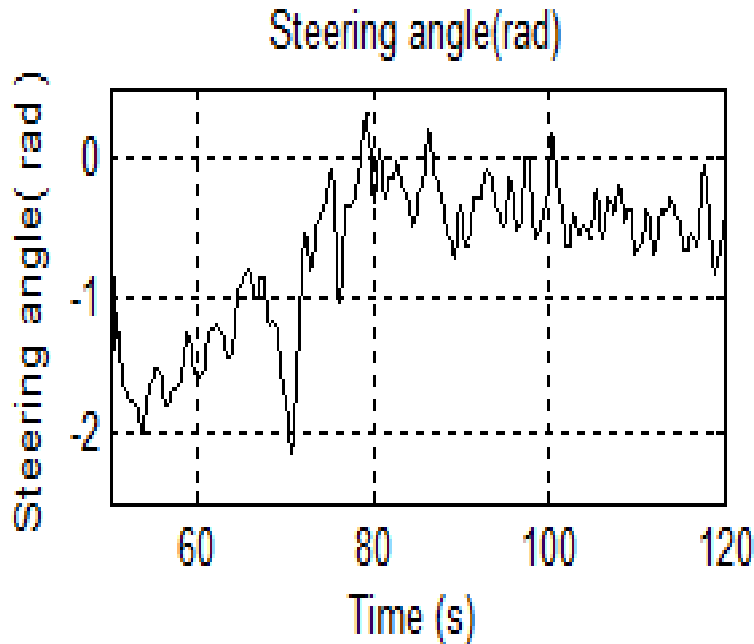


Figure 6. Steering-Wheel Angle

3. Results and Analyzes

In this part, we use real entered signals of the road provided by IFSTTAR for three types of lanes (dry, wet, glaze), the vehicle rolls at a mean velocity of 50km/h.

In what follows we will represent the effect of the three tracks on the simulated dynamic behavior of the vehicle taking in account the orders of driver, the plan of the road represented by the angles of Euler Rolling-Pitching-Yaw (ψ_x, ψ_y, ψ_z) as illustrated previously and the forces of the contacts given by the formula of Pacejeka[13].

3.1. Effects on the Side and Longitudinal Slip

Figure 7 illustrates the evolution of the sideslip angle of the left front steerable wheel and their longitudinal slip in time for the three types of tracks.

It is note that, the sideslip angle of left front wheel follows the steering-wheel angle given by Figure 6, with a certain shift in the negative direction for the wet tracks, in the case of the two phases of steering. In the case of longitudinal slip, it is noted that the longitudinal slip almost reached 5% during the first phase of steering and then it returns to a value lower than 1% and there remains stable around this value.

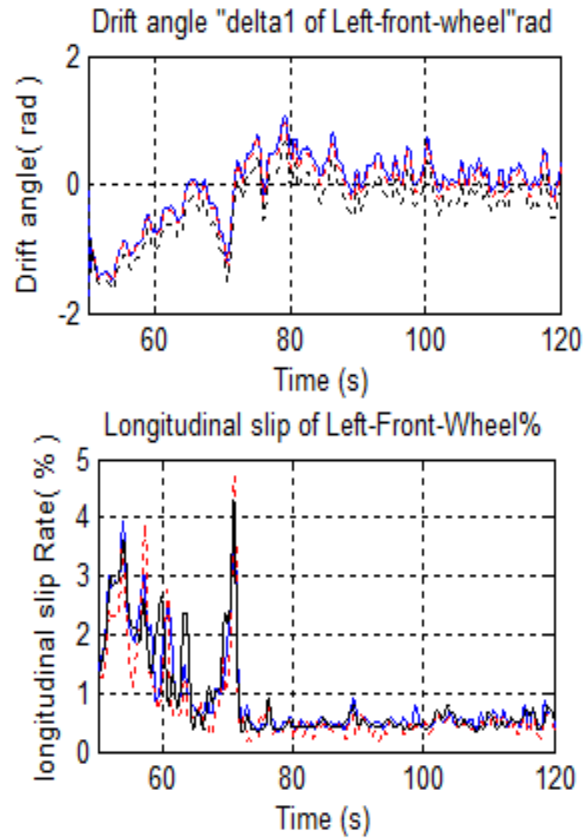


Figure 7. Effect Tracks to the Drift Angle and Longitudinal Slip Ratio (Bleu-dry Lane, Red-wet lane and Black-glaze Lane)

3.2. Effects on the Wheels Velocities

We illustrated in figure 8 the case of left front steerable wheel to clear up the effect of the three tracks on linear and rotations velocities of the wheel.

It is well observed that the rotation velocity is around 52 rad/s in the case of the track dry and wet what translates that linear velocity is around 14 m/s. But in the case of the track glaze it is observed that speeds in extreme cases tend to be annulled. What explains why the vehicle starts to enter a total slip.

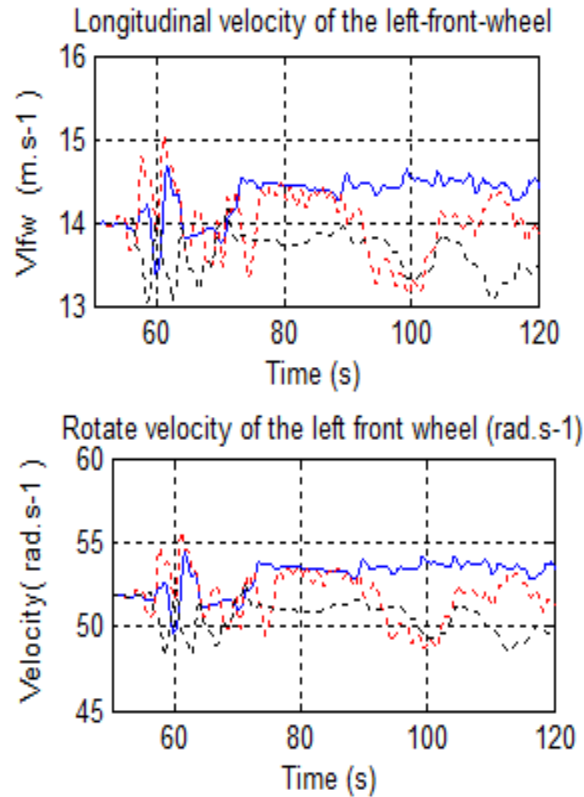


Figure 8. Effect Tracks on the Linear and Rotations Velocities of the Wheels (Bleu-dry Lane, Red-wet Lane and Black-glaze Lane)

3.3. Effects on the Suspensions of the Four Wheels

The effects of three tracks on the clearance acceleration at suspensions are given by Figure 9. It is noted that in the dry track case, the acceleration is proportional to the plan of road given by figure 5 on the other hand in the case of the wet track and glaze the acceleration of clearance in the course of time tends to increase this. This is translated by a fast increase in clearances of the suspensions. Indeed this increase influences directly the stability of the vehicle.

3.4. Effects on the Chassis

We represented here the effect of adherence on longitudinal, side and vertical acceleration of the chassis given by Figure 10 and one represented their effect on the angles of orientation of the chassis given by the angles rolling-pitching-yaw illustrated by Figure 11.

It is noticed that:

- Longitudinal acceleration, decrease with each increase of the rate of humidity.
- The side and the vertical clearances acceleration increase with each increase of the rate of humidity.

One can say from some remarks that the vehicle with each increase in the rate of humidity in the course of time tends to slip into the longitudinal direction and to deviate laterally with more clearances vertically.

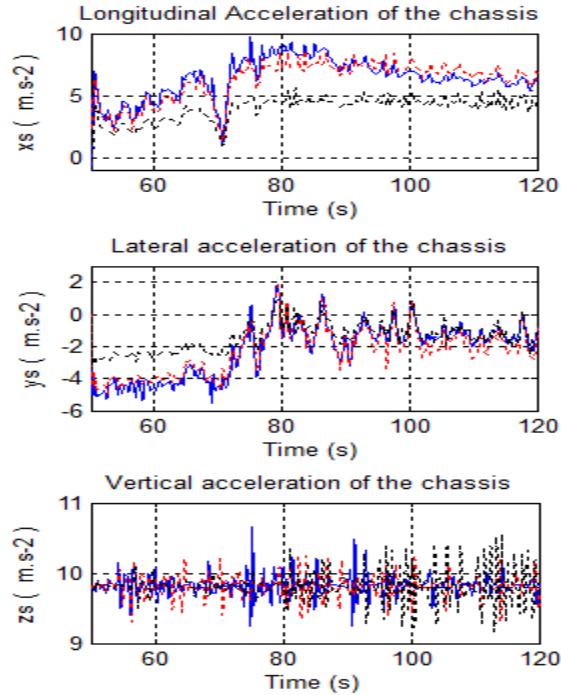


Figure 10. Effect Tracks on the Acceleration Longitudinal, Lateral and Vertical (Bleu-dry Lane, Red-wet Lane and Black-glaze Lane)

On Figure 11 one observes that the angles rolling-pitching-yaw tend to this diverged in time with each increase from the rate humidity.

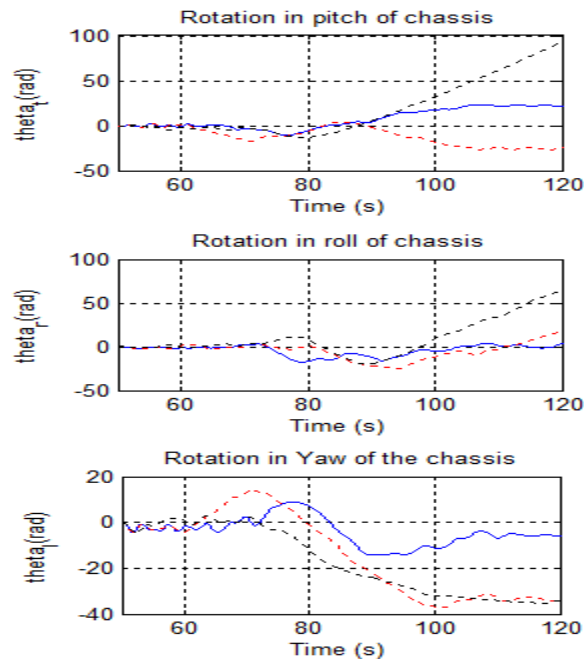


Figure 11. Effect Tracks on the Roll-pitch-yaw Angles (Bleu-dry Lane, Red-wet Lane and Black-glaze Lane)

3.5. Effects on the Generalized Forces Contacts of the Wheels

The curves of evolution in the time of the generalized longitudinal, side and vertical forces in the space articulated according to the nature of track as given by Figure 12.

It is noted that:

- The component resulting from the generalized longitudinal and vertical force decrease, with each increase for the rate humidity
- The component resulting from the generalized side force increases with each increase for the rate humidity.

Finally, we can note that the dynamic behavior of the vehicle depends absolutely on the nature of coating of the track on which the vehicle runs.

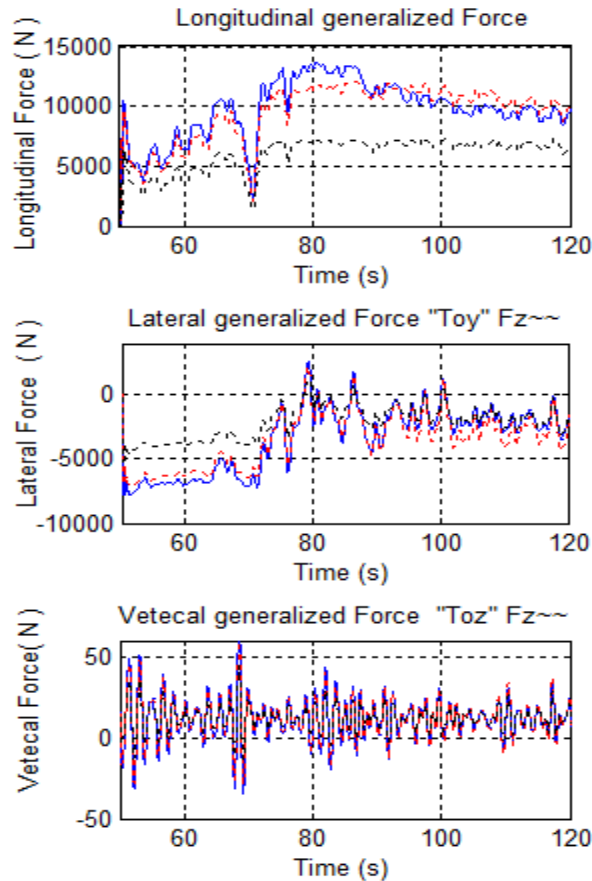


Figure 12. Effect Tracks on the Gneral Forces Longitudinal, Lateral and Vertical (Bleu-dry lane, Red-wet lane and Black-glaze Lane)

4. Conclusion

We proposed in this paper a simulator of a nominal model of the road vehicle rather near to the real physical system, which makes it possible to describe its dynamics. Consequently, we based on signals of input real of the road to describe the influence of adherence on the dynamic behavior of the vehicle.

We represented like results of the effects of adherence according to water content's on the longitudinal, sideslip, and speed of the wheels, clearance of the suspensions, orientation of the frame and on the generalized forces of contacts wheels-ground.

This simulator can be wide while inserting new components to see their influence on the vehicle handling; it will be also useful for the design of laws of command for the control of the vehicle.

Appendix: Parameters of the models

❖ Inertia matrix of the system

$M(q)(16 \times 16) =$

m11	0	0	m14	m15	m16	m17	m18	m19	m1,10	0	0	0	0	0	0
0	m22	0	m24	m25	m26	m27	m28	m29	m210	0	0	0	0	0	0
0	0	m33	0	m35	m36	m37	m38	m39	m310	0	0	0	0	0	0
m41	m42	0	m44	m45	m46	m47	m48	m49	m410	m411	m412	m413	m414	m415	m416
m51	m52	m53	m54	m55	m56	m57	m58	m59	m510	m511	m512	m513	m514	m515	m516
m61	m62	m63	m64	m65	m66	m67	m68	m69	m610	0	0	0	m614	m615	m616
m71	m72	m73	m74	m75	m76	m77	0	0	0	0	0	0	0	0	0
m81	m82	m83	m84	m85	m86	0	m88	0	0	0	0	0	0	0	0
m91	m92	m93	m94	m95	m96	0	0	m99	0	0	0	0	0	0	0
m101	m102	m103	m104	m105	m16	0	0	0	m1010	0	0	0	0	0	0
0	0	0	m411	m511	0	0	0	0	0	m1111	0	0	0	0	0
0	0	0	m412	m512	0	0	0	0	0	0	m1212	0	0	0	0
0	0	0	m413	m513	0	0	0	0	0	0	0	m1313	0	0	0
0	0	0	m414	m514	m614	0	0	0	0	0	0	0	m1414	0	0
0	0	0	m415	m515	m615	0	0	0	0	0	0	0	0	m1515	0
0	0	0	m416	m516	m616	0	0	0	0	0	0	0	0	0	m1616

❖ Coriolis and Centrifuges terms matrix:

$C(q, \dot{q})(16 \times 16) =$

0	0	0	C14	C15	C16	C17	C18	C19	C1,10	0	0	0	0	0	0
0	0	0	C24	C25	C26	C27	C28	C29	C210	0	0	0	0	0	0
0	0	0	0	C35	C36	C37	C38	C39	C310	0	0	0	0	0	0
0	0	0	C44	C45	C46	C47	C48	C49	C410	C411	C412	C413	C414	C415	C416
0	0	0	C54	C55	C56	C57	C58	C59	C510	C511	C512	C513	C514	C515	C516
0	0	0	C64	C65	C66	C67	C68	C69	C610	C611	C612	C613	C614	C615	C616
0	0	0	C74	C75	C76	0	0	0	0	0	0	0	0	0	0
0	0	0	C84	C85	C86	0	0	0	0	0	0	0	0	0	0
0	0	0	C94	C95	C96	0	0	0	0	0	0	0	0	0	0
0	0	0	C104	C105	C106	0	0	0	0	0	0	0	0	0	0
0	0	0	C114	C115	C116	0	0	0	0	0	C1112	C1113	0	0	0
0	0	0	C124	C125	C126	0	0	0	0	C1211	0	0	0	0	0
0	0	0	C134	C135	C136	0	0	0	0	C1311	0	0	0	0	0
0	0	0	C144	C145	C146	0	0	0	0	0	0	0	0	0	0
0	0	0	C154	C155	C156	0	0	0	0	0	0	0	0	0	0
0	0	0	C164	C165	C166	0	0	0	0	0	0	0	0	0	0

❖ The form symbolic system of the jacobian matrix of the four points of contact (wheels) is:

$J^T(16 \times 12) =$

1	0	0	1	0	0	1	0	0	1	0	0
0	1	0	0	1	0	0	1	0	0	1	0
0	0	1	0	0	1	0	0	1	0	0	1
J41	J42	0	J44	J45	0	J47	J48	0	J410	J411	0
J51	J52	J53	J54	J55	J56	J57	J58	J59	J510	J511	J512
J61	J62	J63	J64	J65	J66	J67	J68	J69	J610	J611	J612
J71	J72	J73	0	0	0	0	0	0	0	0	0
0	0	0	J84	J85	J86	0	0	0	0	0	0
0	0	0	0	0	0	J97	J98	J99	0	0	0
0	0	0	0	0	0	0	0	0	J1010	J1011	J1012
0	J112	0	0	0	0	0	0	0	0	0	0
0	0	0	0	J125	0	0	0	0	0	0	0
J131	0	0	0	0	0	0	0	0	0	0	0
0	0	0	J144	0	0	0	0	0	0	0	0
0	0	0	0	0	0	J157	0	0	0	0	0
0	0	0	0	0	0	0	0	0	J1610	0	0

References

- [1] J. Villagra, B. d’Andrea- Novel, M. Fliess and H. Mounter, “A diagnostic-based approach for tire-road forces and maximum friction estimation”, In Control Engineering Practicem, (2010).
- [2] S. Muller, M. Uchanski and K. Hedrick, “Estimation of the Maximum Tire-Road Friction Coefficient”, Journal of Dynamic Systems, Measurement, vol. 125 / 607, (2003).
- [3] H. Fischein, R.Gnadier, H.Unrau, “The Influence of the Track Surface Structure on The Frictional Force Behaviour of Passenger Car Tyres in Dry and Wet Track Surface Conditions”, ATZ, vol. 10, (2001), pp. 950-962.
- [4] H. Imine, L. Fridman, H. Shraim, and M. Djemai, “Sliding Mode Based Analysis and Identification of Vehicle Dynamics”, Lecture Notes in Control and Information Sciences, Library of Congress Control Number: 2011932321, (2011); Springer-Verlag Berlin Heidelberg.
- [5] J. J. Craig. Introduction to robotics: Mechanics and control. Addison- Wesley, (1989).
- [6] W. Khalil and E DombreModelling, “Identification and control of robots”, Hermès Penton, (2002), London & Paris.
- [7] A. El Hadhri, “Modélisation de véhicules, observation d’état et estimation des forces pneumatiques : Application au contrôle longitudinal”, Thèse de doctorat, Université de Versailles-Saint-Quentin en Yvelines, (2001).
- [8] B. Zami, “Contribution à l’identification de la liaison Véhicule-Sol d’un véhicule automobile Estimation des paramètres de modèles depneumatiques”, PhD thesis, Université de Haute-Alsace, (2005).
- [9] M. Oudghiri, "Commande multi-modèles tolérante aux défauts :Application au controle de la dynamique d'un véhicule automobile", doctorat de université de picardie jules verne, Université de picardie jules verne, (2008).
- [10] O. Orfila, "Influence de l’infrastructure routière sur l’occurrence des pertes de contrôle de véhicules légers en virage : modélisation et validation sur site expérimental", Thèse de doctorat, Université D’Evry-Val-d’Essone, (2009).
- [11] S. Maakaroun , "Modélisation et simulation dynamique d’un véhicule urbain innovant en utilisant le formalisme de la robotique", Thèse de doctorat, Université de Nantes angers le mans, (2011).
- [12] M. Ouahi, "Observation de système à entrées inconnues, applications à la dynamique automobile", Thèse de doctorat, Université de Limoges, (2011).
- [13] H.B. Pacejka., Besseling, Magic Formula Tyre Model with Transient Properties. 2nd International Tyre Colloquium on Tyre Models for Vehicle Dynamic Analysis, (1997); Berlin, Germany.
- [14] N. Hamadi, H. Imine et D.-E. Ameddah, "Outils Principaux Pour le Développement d’un Modèle de Véhicule articulé tout Terrain", International Conference on Syatems and Processing Information, (2013); Guelma, Algeria.
- [15] N. K. M’Sirdi, B. Jaballah, A. Naamane and H. Messaoud, “Robust Observers and Unknown Input Observers for estimation, diagnosis and control of vehicle dynamics”, IROS, (2008); NICE, France.

Authors



Nacer Hamadi, received the Engineering degrees in Control for electronically engineering from the Batna University, Algeria, in 1995. Later, he has been working for 10 years as state engineer of the laboratories in the University of Constantine, Algeria and he has received the Magister in Robotics for electronically engineering at this period. Currently he has doctoral student in the field of robotics. His main research interests include dynamics and control of a robots and vehicle ground.



Djamel-eddine Ameddah, received the Masters degrees in electronics engineering from the National Polytechnic School of El-Harrach, Algeria, in 1984. Holds his Ph.D in Electrical Engineering obtained from collaboration between Algerian and French Universities in 2004. He has been responsible of the undergraduate program in the engineering school for many years. He was involved or leading several research projects including the actual project: ‘modeling and control of wheeled mobile robots’. His research interests include robotics, traction control systems, mechatronics.



Hocine Imine, received the Master’s degree and the Ph.D. degree in robotics and automation from Versailles University, Versailles, France, in 2000 and 2003, respectively. From 2003 to 2004, he was a Researcher with the Robotic Laboratory of Versailles (LRV in French) and an Assistant Professor with Versailles University. In 2005, he joined Institut Français des Sciences et Technologies des Transports, where he is currently a Researcher. He received the Accreditation to Supervise Research (Habilitation à Diriger des Recherches—HDR) in March 2012. He is involved in different projects like véhicule interactif du futur (VIF) and heavy route (intelligent route guidance for heavy traffic). He is also responsible for the research project PLInfra on heavy vehicle safety and the assessment of their impacts on pavement and bridges. He has published two books, over 60 technical papers, and several industrial technical reports. His research interests include intelligent transportation systems, heavy vehicle modeling and stability, diagnosis, nonlinear observation, and nonlinear control.

